SAND2022-8853C

Mesoscale simulations of pressure-shear loading of a granular ceramic

Brian Demaske,
Sandia National Laboratories

Sandia National Laboratories is a multi-mission laboratory managed and operated by National Technology & Engineering Solutions of Sandia, LLC, a wholly owned subsidiary of Honeywell International Inc., for the U.S. Department of Energy's National Nuclear Security Administration under contract DE-NA0003525.

Sandia National Laboratories is a multimission laboratory managed and operated by National Technology & Engineering Solutions of Sandia, LLC, a wholly owned subsidiary of Honeywell International Inc., for the U.S. Department of Energy's National Nuclear Security Administration under contract DE-NA0003525.

Introduction and Motivation

- Important to understand how granular ceramics respond under high strain rates
- Mesoscale models for granular materials used in hydrocodes to simulate normal plate impact tests
  - First applied to metal powders and more recently to ceramic powders
  - Good success in describing compaction response despite brittle nature of ceramics
- Goal of this work to investigate how mesoscale models for granular ceramic materials perform during shear loading
- Build upon work by LaJeunesse[1] modeling pressure-shear tests on sand
- Use granular WC as additional experiments[2] against which to compare simulation results

[1]LaJeunesse, J. W. (2018). Dynamic Behavior of Granular Earth Materials Subjected to Pressure-shear Loading, Marquette University. PhD Dissertation.
[2]Vogler, T.J., et al. (2011). Pressure-shear experiments on granular materials. Sandia National Laboratories (SAND2011-6700)

Details of Mesoscale Simulations

- Simulate pressure-shear tests using Sandia's shock physics code CTH
  - Initial flyer velocity: $u_0 = V\cos(\theta)$ and $v_0 = V\sin(\theta)$
- Flyer and anvils modeled as elastic with properties of Ti-6Al-4V
- Powder sample modeled as random packing of spherical grains
  - Grain size of 25 μm and packing fraction of 65%
- Mie-Grüneisen EOS, elastic perfectly plastic strength model, and cap on tensile pressure to model fracture
- CTH slide algorithm as an alternative to default mixed-cell treatment

Property	WC	Ti-6Al-4V
initial density ρ_0 (g/cc)	15.56	4.415
sound speed C_S (km/s)	5.26	4.91
U_S-u_p Hugoniot slope	1.15	-
Grüneisen parameter	1.0	-
Specific heat (J/kg.K)	172	-
Yield stress Y_0 (GPa)	5	-
Poisson ratio ν	0.2	0.317
Fracture strength σ_{fs} (GPa)	4.0	-

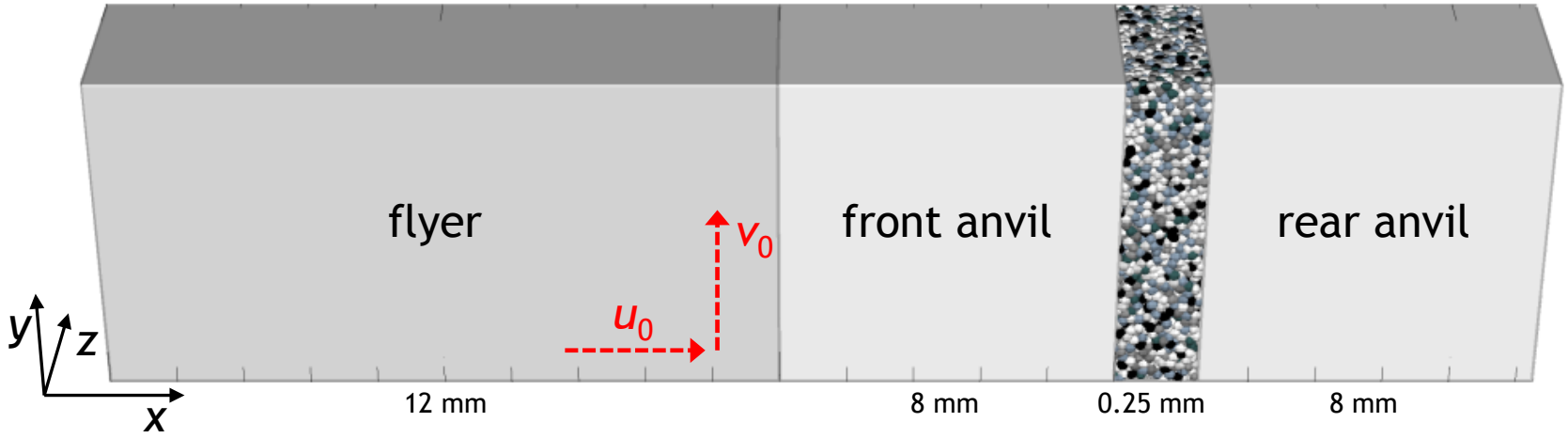

Comparison of Simulated and Experimental Velocity Histories

- Simulations at same initial conditions as in experiment: $\theta = 20°$ and $V = 66$, 121 and 145 m/s
- More rapid initial rise of normal velocity in simulations – less compaction
  - Reduced with intergranular sliding, but still higher than experiment
- Smooth rise in transverse velocity to steady level
  - Default mixed-cell treatment ~v_0
  - Reduced with intergranular sliding enabled, however no macroscopic shear flow
  - Some localized flow at grain interfaces that is exacerbated at low impact velocities

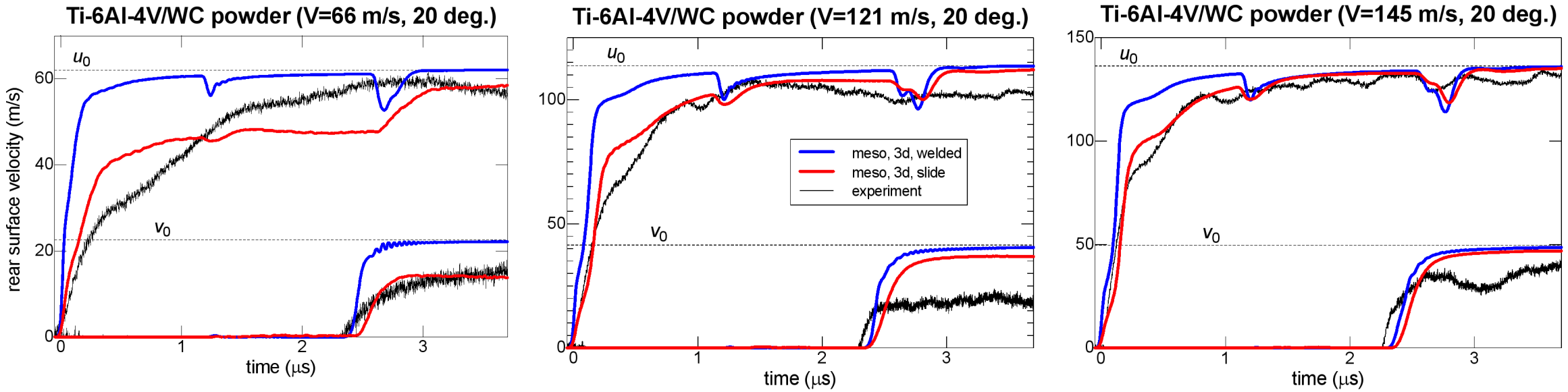

Probing the Shear Failure Surface of the Mesoscale Powder Model

- Adjust V and θ to generate shear waves of increasing amplitude τ_{el}, while keeping normal wave amplitude σ_{el} fixed

$$V = \frac{2\sigma_{el}}{\rho_{0,A} C_{L,A}} \left[1 + \left(\frac{C_{L,A}\tau_{el}}{C_{S,A}\sigma_{el}} \right)^2 \right]^{1/2} \quad \text{and} \quad \theta = \tan^{-1}\left(\frac{C_{L,A}\tau_{el}}{C_{S,A}\sigma_{el}} \right)$$

- Varied τ_{el} from 1 to 2 GPa, while σ_{el} fixed at 0.838 GPa
- Simulations with welded grains respond elastically (not shown)
- Simulations with intergranular sliding show transmitted transverse velocity is bounded
- Transverse velocity increases over time, as grains rearrange
- Drop in velocity due to formation of a sliding interface within the sample

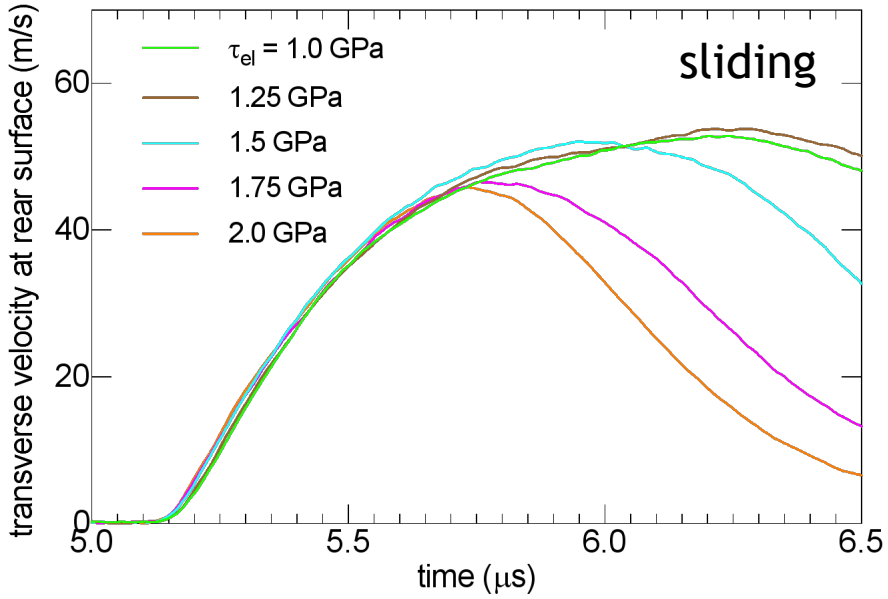

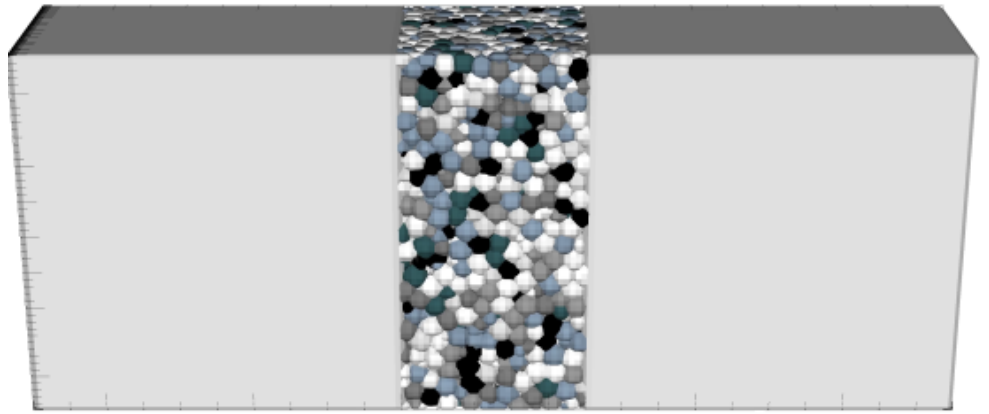

cells colored by plastic strain of WC

Effect of Intragranular Fracture Strength

- Very few cells reach fracture criterion, while recovered samples in experiment show evidence of significant grain fracture
- Switch to a principal-stress-based fracture criterion and decrease fracture strength from its baseline value of 4 GPa
- Determine upper bounds in normal and transverse velocity histories fixing σ_{el} = 0.838 GPa and varying τ_{el} = 0.25-2 GPa
- Reduction in initial shoulder of normal wave rise with decreasing fracture strength
  - Indicates more compaction during initial rise, which is in better agreement with experiment
- Upper bound in transverse velocity decreases with decreasing fracture strength
  - Lower limit for fracture strength 0.25-0.5 GPa
  - Below that the upper bound increases

normal stress = 0.838 GPa

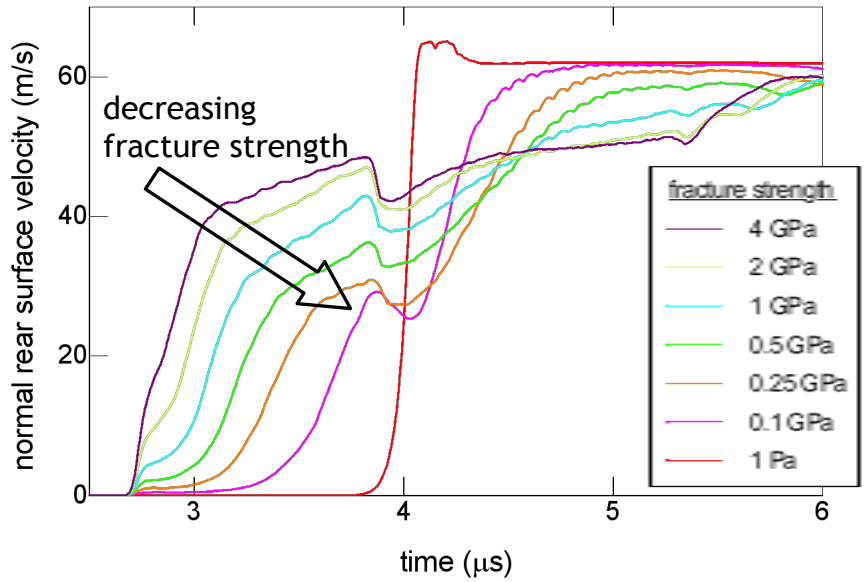

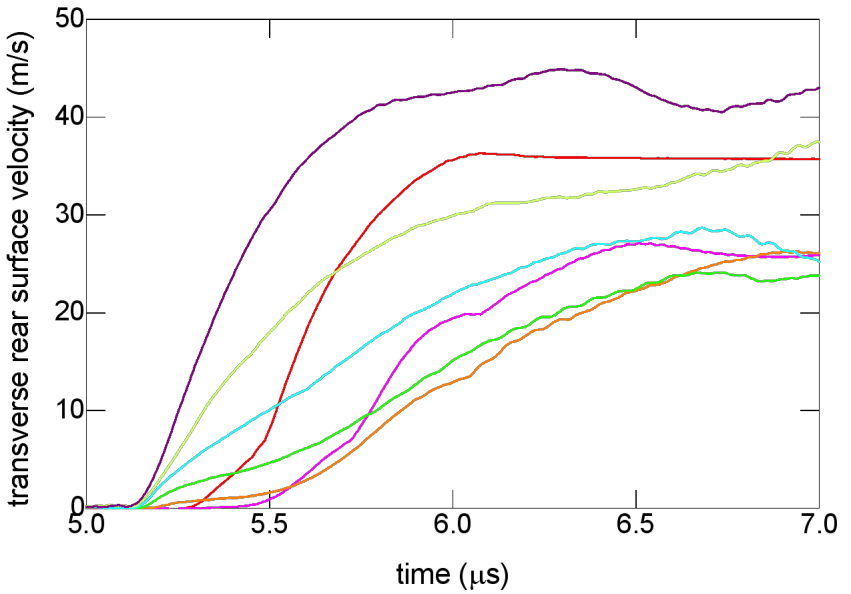

Conclusions

- Simulated pressure-shear loading of granular WC using simple mesoscale model for powder
- Found essentially an elastic shear response at experimental impact conditions
- Shear failure behavior of mesoscale powder model depends strongly on mixed-cell treatment and intragranular fracture strength
- Issues with slide algorithm leading to nonphysical behavior in the form of
  - Localized flow at grain interfaces
  - Formation of internal slide interfaces that span the cross-section of the sample
- Limitation of Eulerian codes to treat contact realistically
- Lagrangian methods may be better suited to modeling these types of problems

Questions?

Extra Slides

Details of Pressure-Shear Test

- Pressure-shear test consists of a flyer with an angled nose and target
- Impact generates both normal and shear waves
- Normal wave reaches sample first – ringing up of normal stress – followed by shear wave
- Multiple PDV probe configuration to measure both normal and transverse velocity components
- Anvils remain elastic, so velocities proportional to average stresses in sample

$$\sigma(t) = \frac{1}{2}(\rho C_L)u(t) \qquad \tau(t) = \frac{1}{2}(\rho C_S)v(t)$$

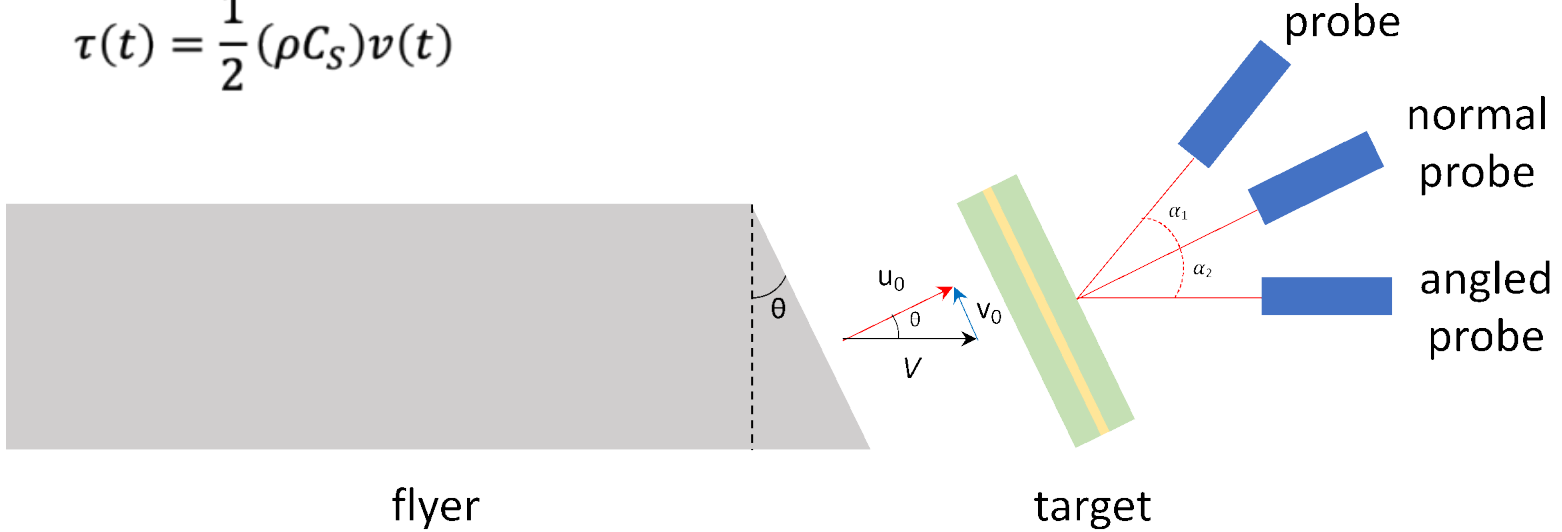

Normal stress states in sample

- Normal impedance (ρc_L) of sample is less than anvils
- Normal waves reverberate inside sample, increasing the normal stress
- Each wave passage compacts the sample, which increases the impedance
- After many reverberations, sample reaches constant normal stress state $\sigma_{el} = \frac{1}{2}(\rho c_L)u_0$
- Since anvils remain elastic, normal stress history in sample can be obtained from the rear anvil free surface
- Normal strain rate given by

$$\dot{\epsilon}(t) = \frac{u_L - u_R}{h_0} = \frac{u_0 - u_{fs}(t)}{h_0}$$

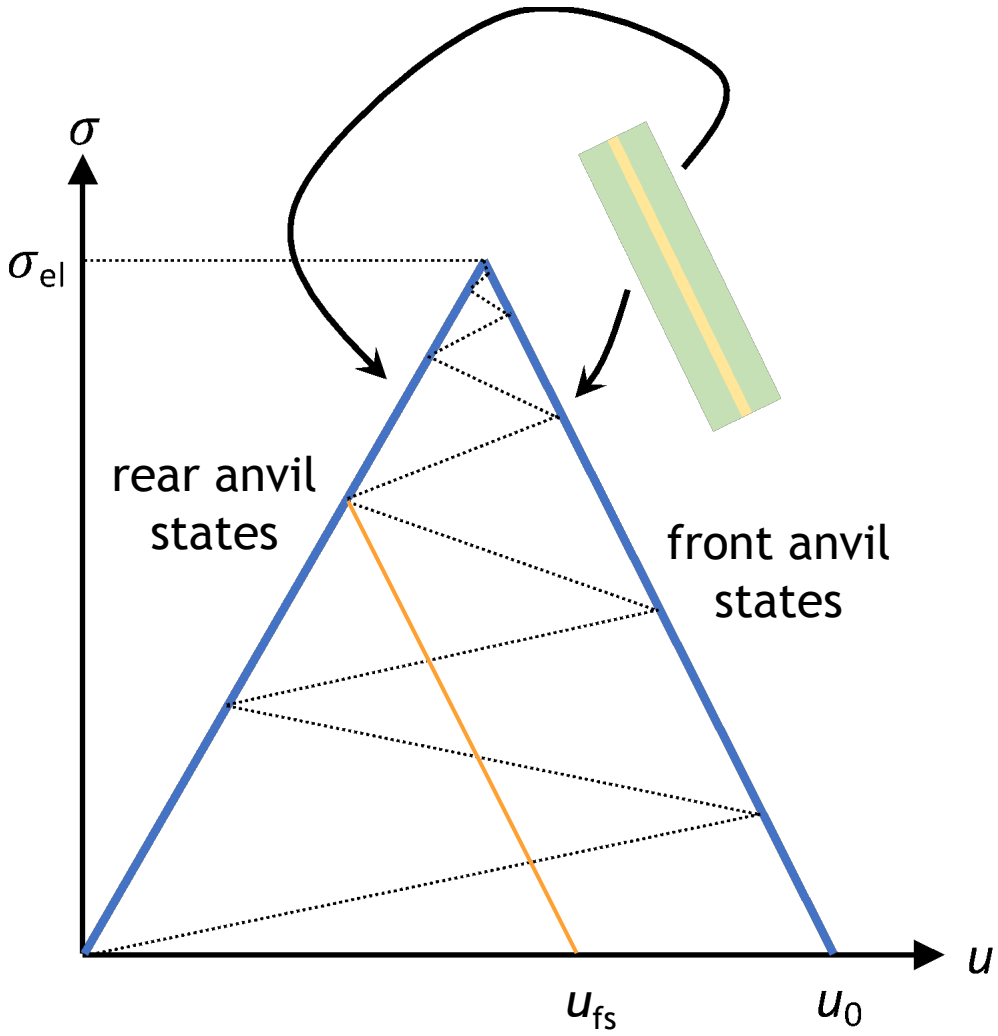

Shear stress states in sample

- Shear impedance (ρc_S) of sample is less than anvils
- Shear waves reverberate inside sample, increasing the shear stress
- After many reverberations, sample reaches constant shear stress state $\tau_{flow} \leq \tau_{el} = \frac{1}{2}(\rho c_S) v_0$
- If $\tau_{flow} < \tau_{el}$, then sample is failing/yielding
- Front and rear anvil interfaces with sample have different transverse velocities
- Shear strain rate given by

$$\dot{\gamma}(t) = \frac{v_L - v_R}{h} = \frac{v_0 - v_{fs}(t)}{h}$$

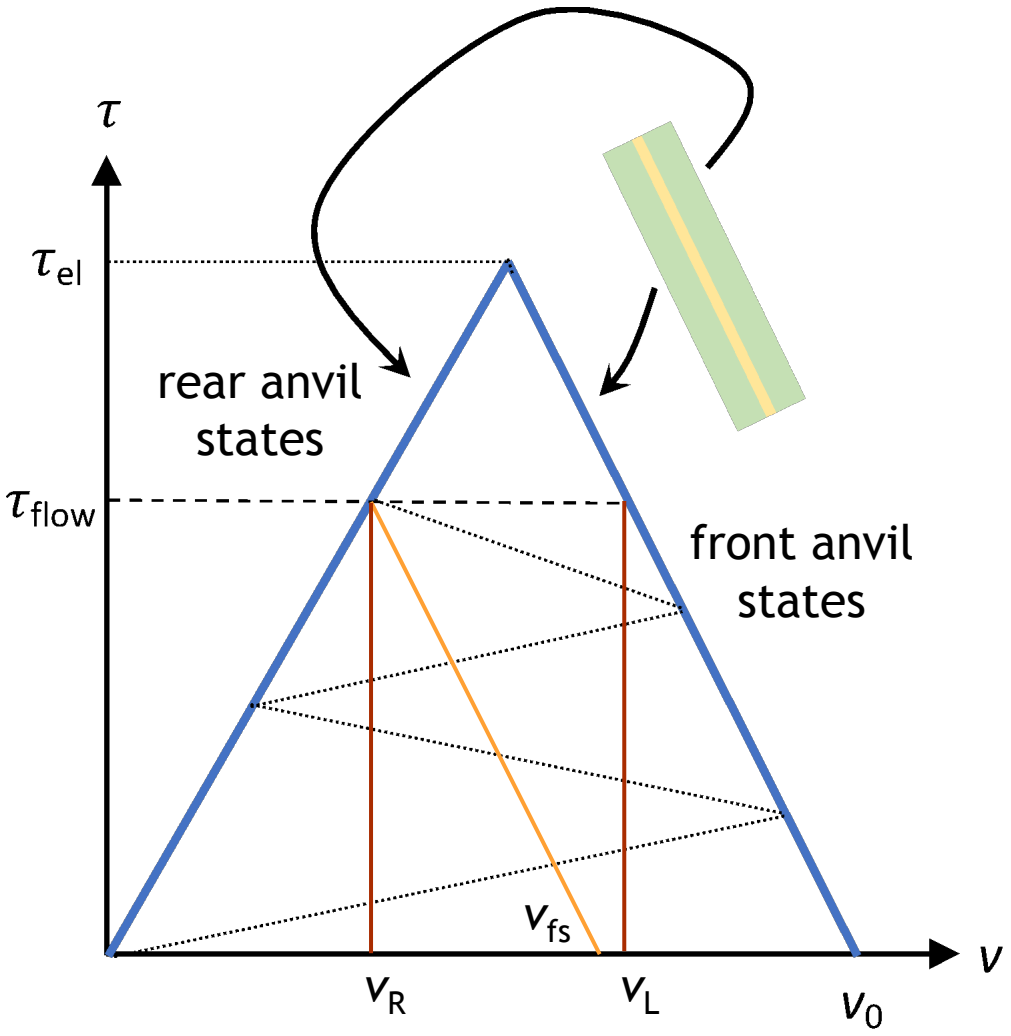

Adaptive mesh refinement

- Grain size determines mesh resolution needed to accurately simulate wave behavior in powder
- Sample occupies only a thin slice of the full model (0.25 mm out of 30 mm total thickness)
  - Therefore, a uniform meshing scheme would waste computational resources simulating high-fidelity wave behavior in flyer/anvils
- Adaptive mesh refinement (AMR) scheme assigns high-resolution mesh to the sample and important interfaces, where it is needed
- Desired sample mesh resolution used to
  the maximum AMR refinement level
- Bulk flyer/anvil regions resolved at 2 leve
  below the maximum refinement level
  - Vacuum regions at lowest refinement level
- AMR indicators keep sample and interfac
  refined at the maximum refinement level
  - Timed indicator to maintain lowest refineme
    until just before normal wave arrives at sam
  - Refined mesh moves with sample/interfaces

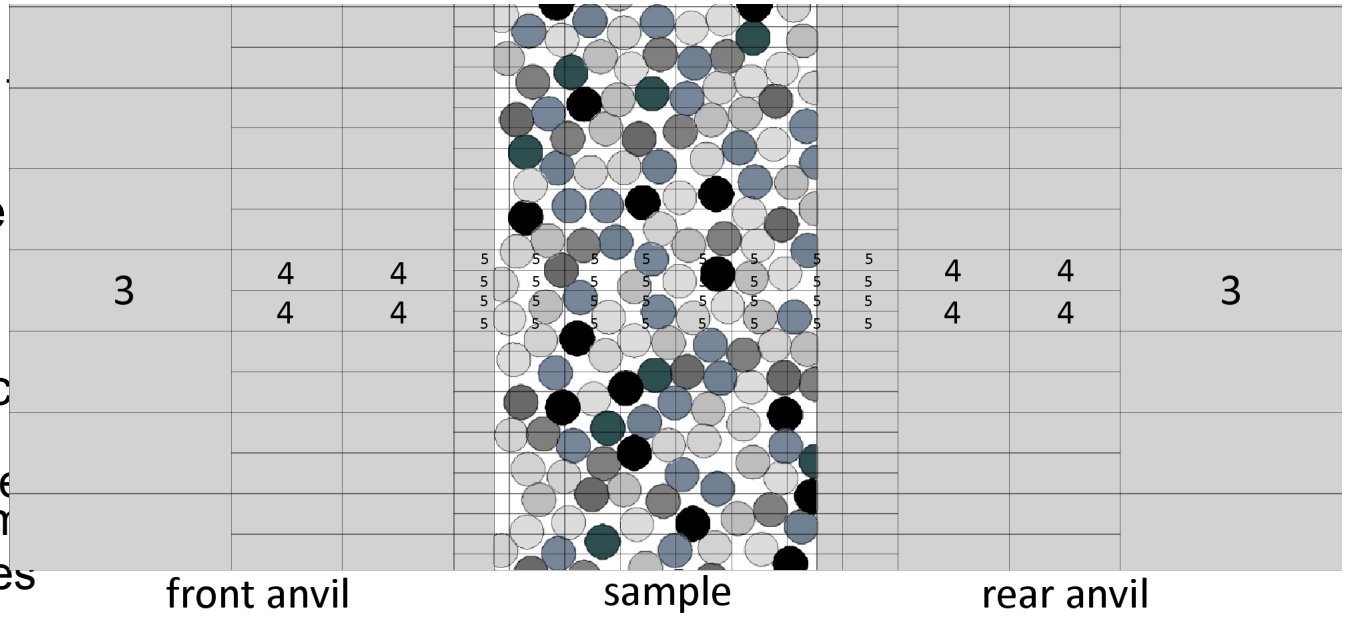

Performance gains for AMR simulations

- Assess performance of AMR calculations compared to a flat mesh calculation performed at resolution corresponding to the maximum AMR refinement level
- Plots show number of AMR blocks and speed-up for 2D and 3D mesh geometries as a function of the refinement level of the flyer/anvils
  - Speed-up defined as flat mesh run time divided by AMR run time
- Highest refinement level corresponds to a mesh resolution of ~2 μm (or ~12 cells/grain for grain size of 25 μm)
- Number of AMR blocks grows exponentially
- AMR calculations with refinement levels of 3 (2D) and 1 (3D) for the flyer/anvil materials, which are each 2 below the maximum refinement level, leads to speed-ups of ~8 and ~5, respectively, over flat mesh calculations

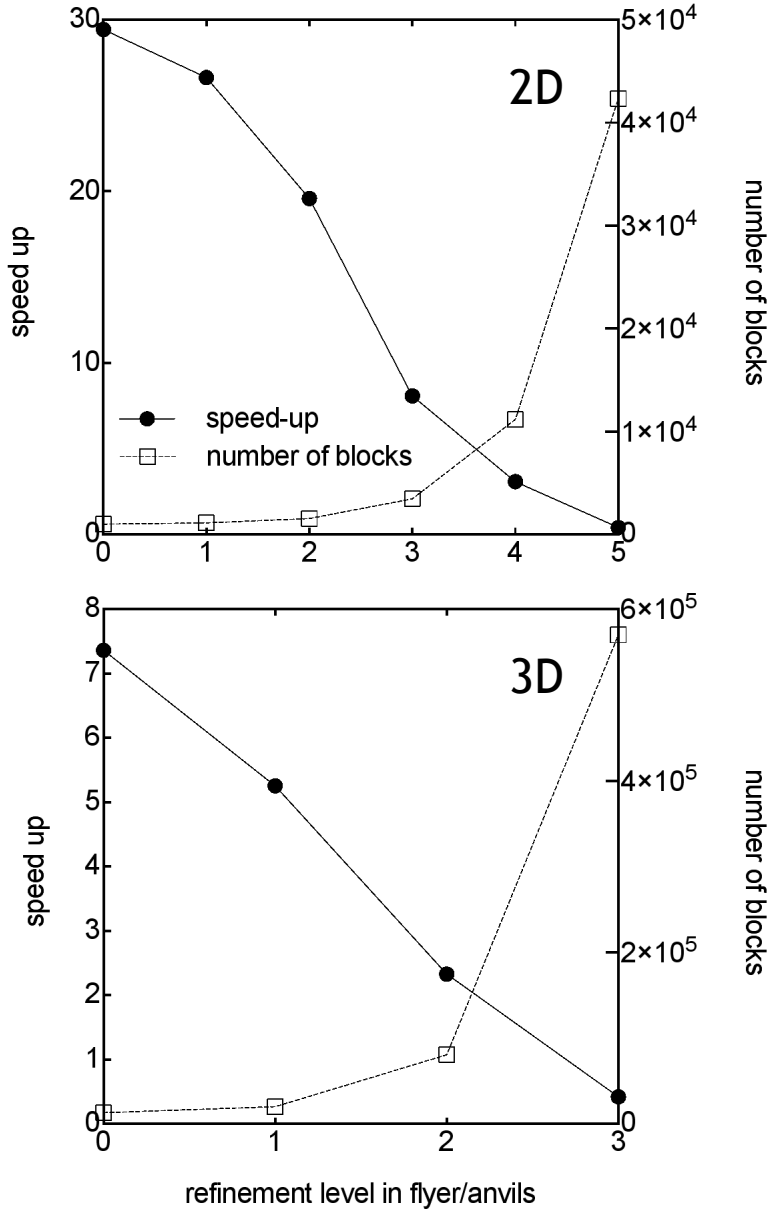

Mesoscale powder generation and slide algorithm enforcement

- Grain realizations generated using granular package of LAMMPS molecular dynamics (MD) code
- Finite-size elastic particles inserted in a box (2D or 3D) with randomized initial positions
  - Particle sizes can be uniform or chosen from a distribution
  - Insertion process terminated once desired volume fraction is reached
- Grain-grain overlap removed using step-size limited MD run
  - Necessary due to large degree of overlap after insertion step
- After initial overlap is removed, particle trajectories are evolved for time it takes for an average particle to travel several mean free path lengths
- Final particle positions and sizes are fed into CTH to generate powder model
- To allow for enforcement of slide algorithm, neighboring grains within a radius of twice the largest grain size are assigned unique material IDs, but given identical material properties
  - Otherwise CTH would treat any grains that were in contact (i.e., belonging to the same mesh cell) as a single continuous volume

Interface motion tracking using Lagrangian tracers

- Planes of tracers placed at front anvil-sample, rear anvil-sample interfaces, and rear anvil free surface
- Motion of these interfaces can be calculated by averaging tracer positions or velocities
- Averaged quantities can be used to compute normal and shear stresses, strains, and strain rates of the sample using the following relationships

$$\epsilon(t) = 1 - \frac{x_r(t) - x_f(t)}{h_{0,x}},\ \dot{\epsilon}(t) = \frac{\dot{x}_f(t) - \dot{x}_r(t)}{h_{0,x}} = \frac{u_0 - \dot{x}_{fs}(t)}{h_{0,x}} \qquad \text{(normal strain, strain rate)}$$

$$\sigma(t) = (\rho C_L)\dot{x}_r(t);\ (\rho C_L)\left(u_0 - \dot{x}_f(t)\right);\ \frac{1}{2}(\rho C_L)\dot{x}_{fs}(t) \qquad \text{(normal stress)}$$

$$\gamma(t) = \frac{y_f(t) - y_r(t)}{x_r(t) - x_f(t)}, \dot{\gamma}(t) = \frac{\dot{y}_f(t) - \dot{y}_r(t)}{x_r(t) - x_f(t)} = \frac{v_0 - \dot{y}_{fs}(t)}{x_r(t) - x_f(t)} \qquad \text{(shear strain, strain rate)}$$

$$\tau(t) = (\rho C_S)\dot{y}_r(t);\ (\rho C_S)\left(v_0 - \dot{y}_f(t)\right);\ \frac{1}{2}(\rho C_S)\dot{y}_{fs}(t) \qquad \text{(shear stress)}$$

Discards for 3D simulations with slide algorithm activated

- With the default settings, 3D simulations with intergranular sliding activated fail after normal wave arrives at the sample, but prior to shear wave arrival
- Failure due to time step falling below the lower bound of 30 ps
- Current simulation time step proportional to the minimum wave propagation time for all mesh cells
- Cell controlling time step at time of failure was almost completely void except for a very small volume fraction ($< 10^{-10}$) of grain material
  - Material was in unphysical thermodynamic state, which led to extremely high sound speed (> 22 km/s)
- Added discard sets to remove material in unphysical thermodynamic states (characterized by temperature, pressure, and sound speed) and any small high-velocity fragments
  - Still exploring minimal discard set needed to keep time step well-behaved
- Leads to removal of ~1.6% of grain material over the simulation duration, which is ~7 μs
  - No removal of flyer/anvil materials

Mesh convergence of simulated velocity histories

- Previous hydrocode analyses using mesoscale powder models used mesh resolutions from 4-12 cells across a grain diameter
- Investigate how sample response depends on mesh size
- Performed 2D mesoscale simulations using a uniform (flat) mesh varying the mesh resolution from 1-20 cells/grain
- Normal velocity is significantly different for mesh resolutions of 1-4 cells/grain, while for resolutions ≥5 cells/grain differences are less significant with very little change above 10 cells/grain
- Transverse velocity shows some irregularities for mesh resolutions of 1-4 cells/grain, but changes little above 5 cells/grain
  - However, no failure of the powder under these impact conditions
- Would be interesting to look at mesh convergence for simulations with slide treatment of grain interfaces and for 3D simulations, though the latter would require using AMR

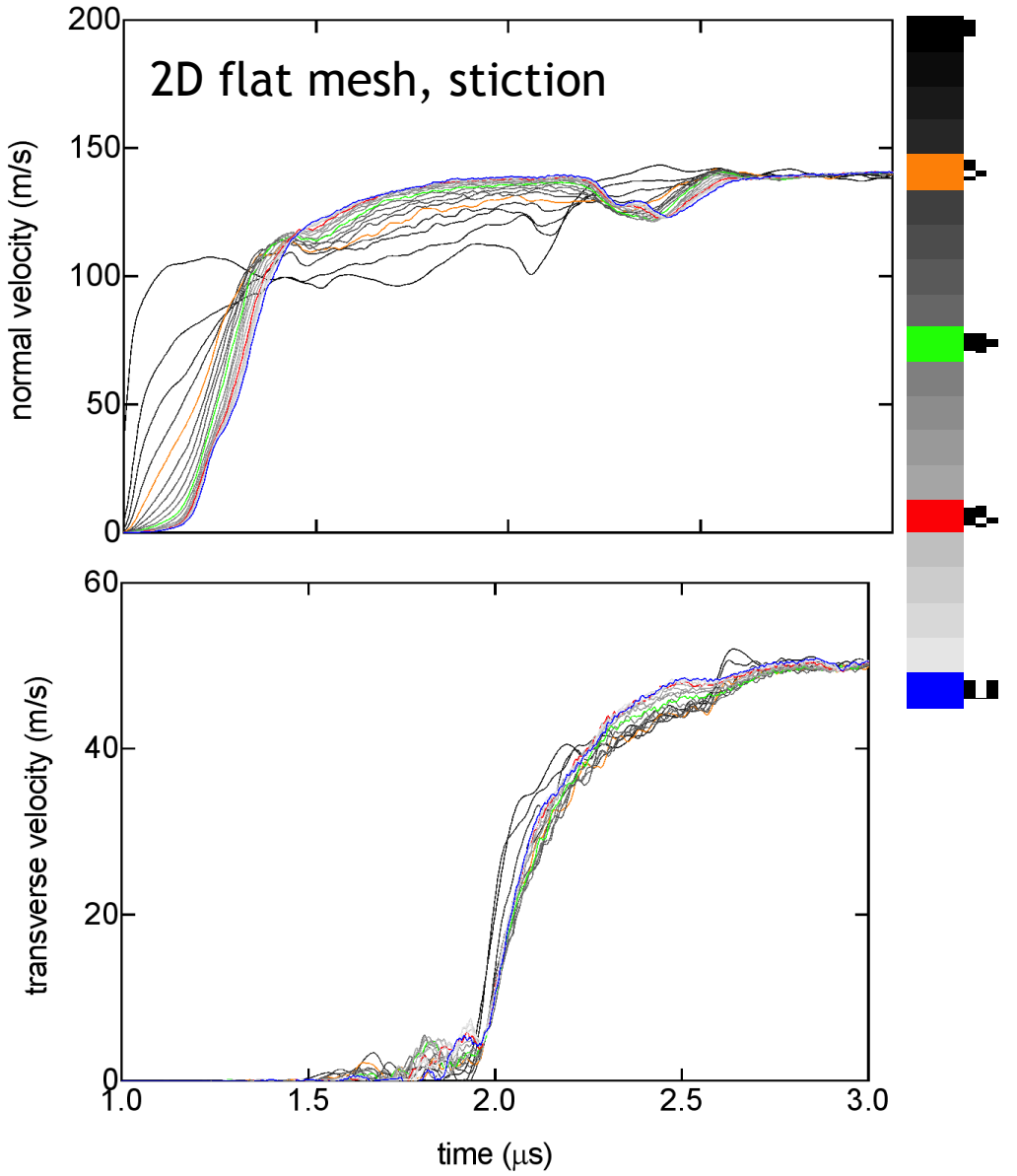

Results of 2D mesoscale simulations

- Simulations match initial normal wave rise, but exhibit steeper rise afterwards indicating less overall compaction than in experiment
  - Slightly more compaction observed when sliding is enforced, but not enough
- Experiments don't reach expected transverse velocity level indicating sample is failing
- Simulations at or near the expected transverse velocity level indicating sample is not failing
  - Transverse velocities for slide simulations are less, but visual inspection shows sample remains intact

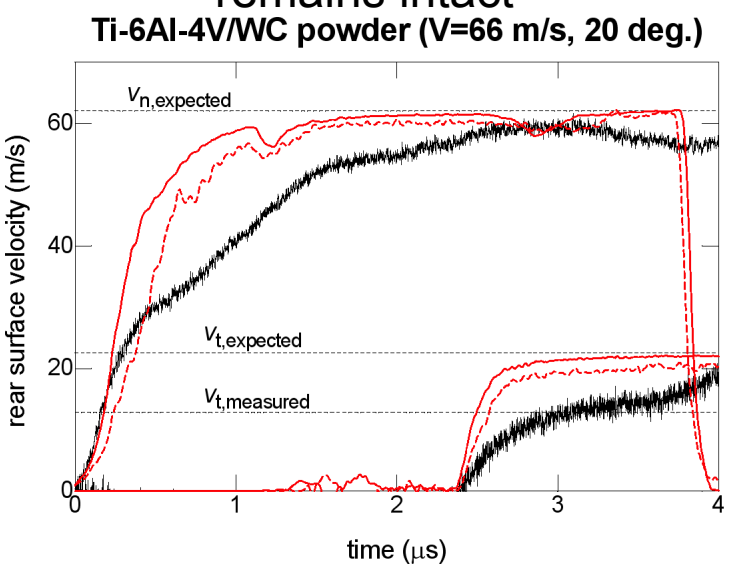

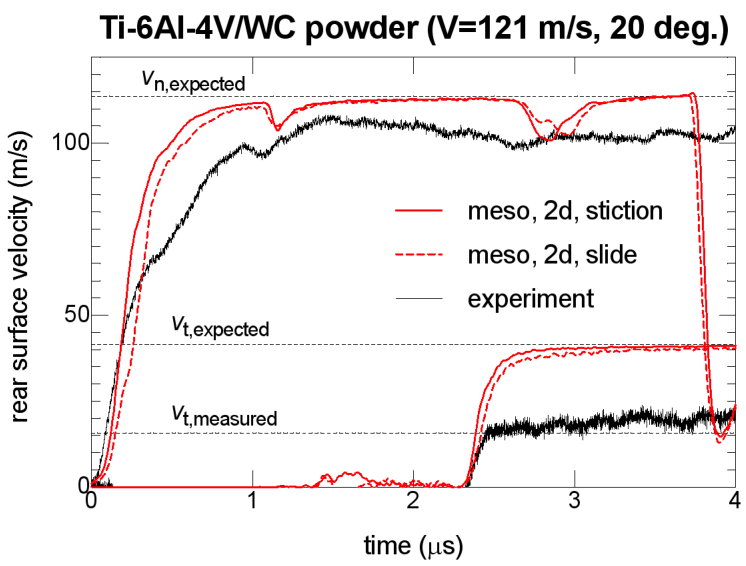

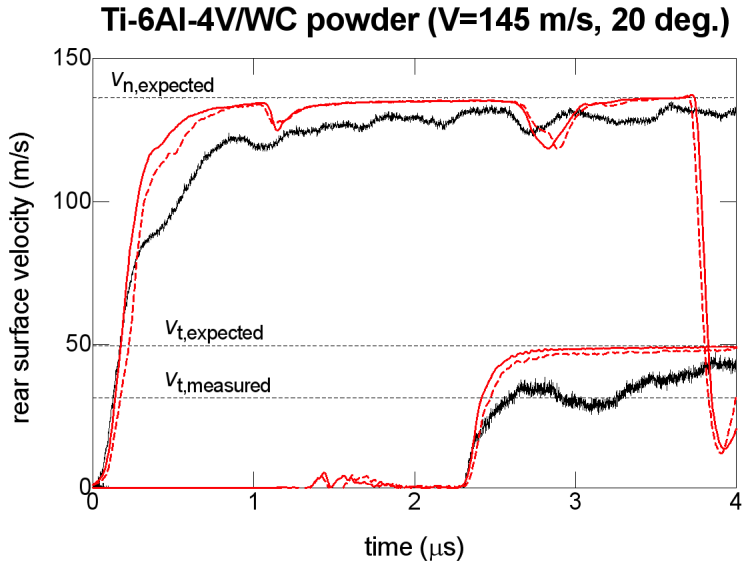

Comparison of Simulated and Experimental Velocity Histories

- Simulations at same initial conditions as in experiment: $\theta = 20°$ and $V = 66$, 121 and 145 m/s
- More rapid initial rise of normal velocity in simulations – less compaction
  - Reduced with intergranular sliding, but still higher than experiment
- Smooth rise in transverse velocity to steady level
  - Default mixed-cell treatment $\sim v_0$
  - Reduced with intergranular sliding enabled, however no macroscopic shear flow
  - Some localized flow at grain interfaces that is exacerbated at low impact velocities

V = 66 m/s

V = 121 m/s

V = 145 m/s

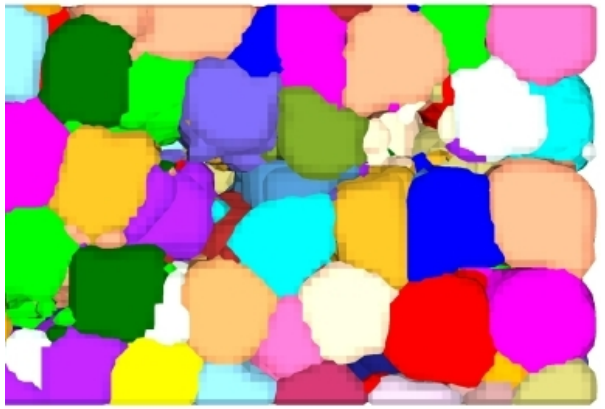

Comparison of Simulated and Experimental Velocity Histories

V = 66 m/s

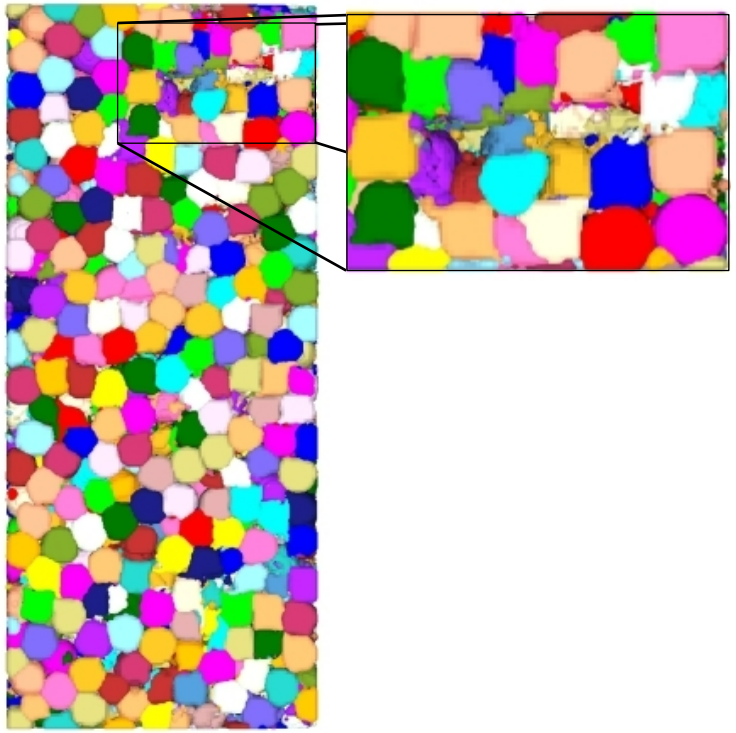

V = 121 m/s

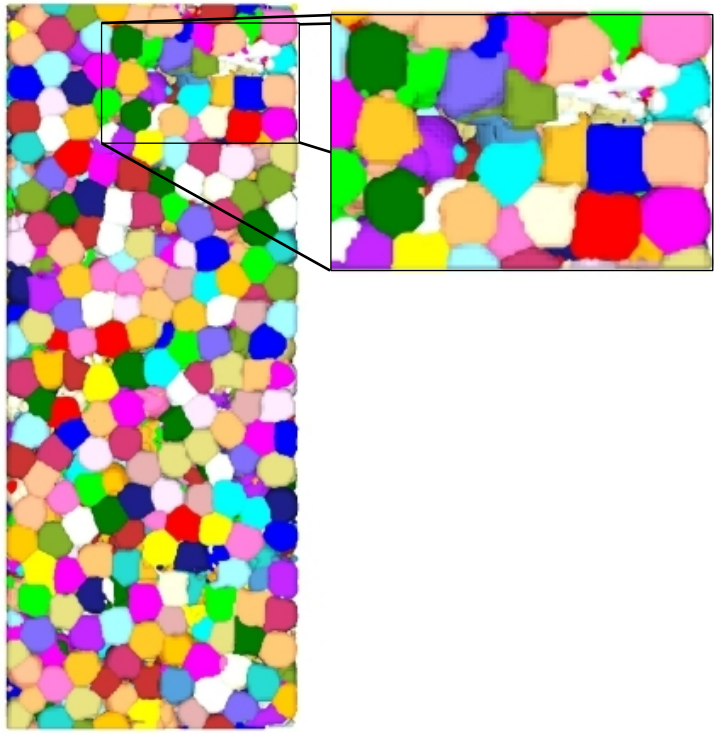

V = 145 m/s

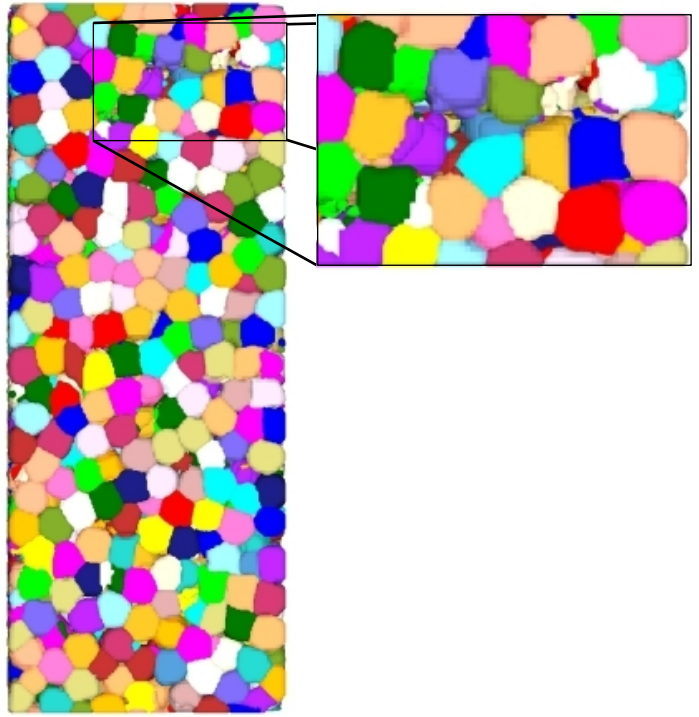

Detailed look at mesoscale simulation results (normal strain rate)

- Normal strain rate for mesoscale simulations and experiments plotted below
  - Compressive strain proportional to area under strain rate curve
- With the exception of the 3D slide simulations, the simulated normal strain rate histories decay more rapidly indicating less overall compaction than observed in experiment
- Strain rate histories for 3D slide simulations agree well with experiment for 121 and 145 km/s cases with the exception of underpredicting the compaction by the initial normal wave
- For the 66 m/s case, the 3D slide simulation overpredicts the experimental strain rate, which may be due to numerical issues with the slide algorithm at low velocities or with the discard sets

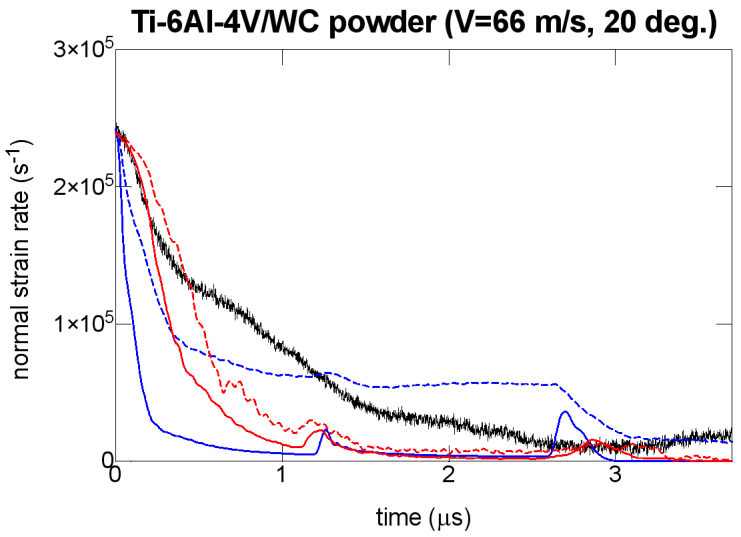

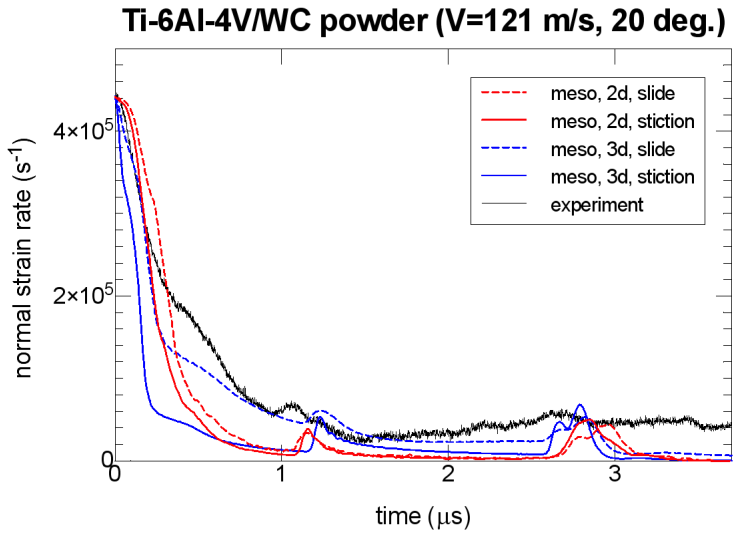

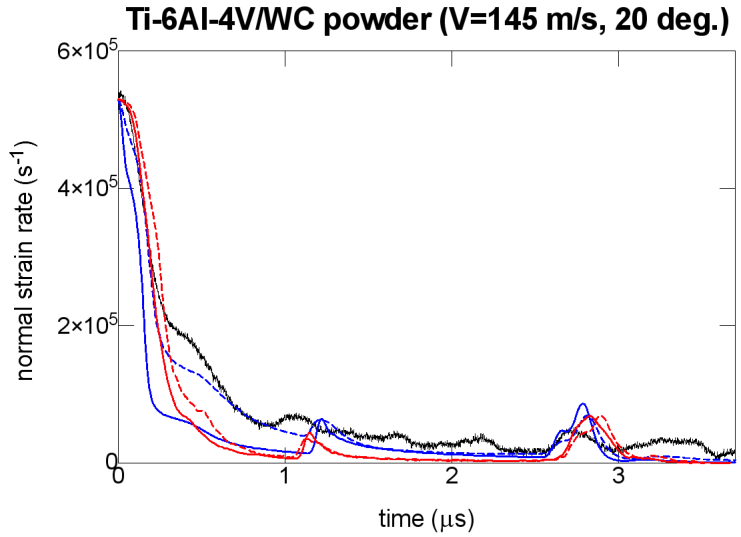

Detailed look at mesoscale simulation results (shear strain rate)

- Experiments show plateau to non-zero strain rate followed by strain-hardening behavior
- In general, simulated strain rate histories show more rapid decay than observed in experiments
  - Shear strain rate for stiction simulations decay to nearly zero after passage of the initial shear wave indicating the powder is not accumulating any significant shear strain (given by area under strain rate curve)
  - Slide simulations exhibit more shear strain accumulation relative to the stiction cases with the difference increasing as impact velocity is lowered
- Visual inspection of the simulated powder sample during the ring up in shear stress and afterwards indicate that the powder is not failing macroscopically, but remains intact and

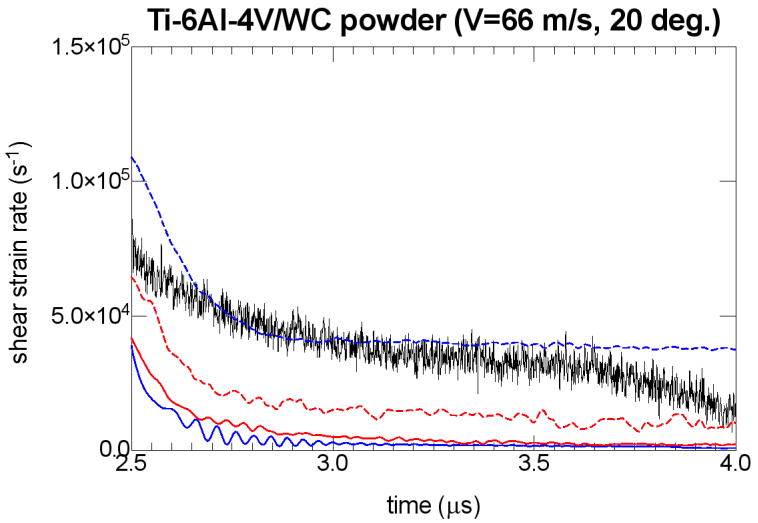

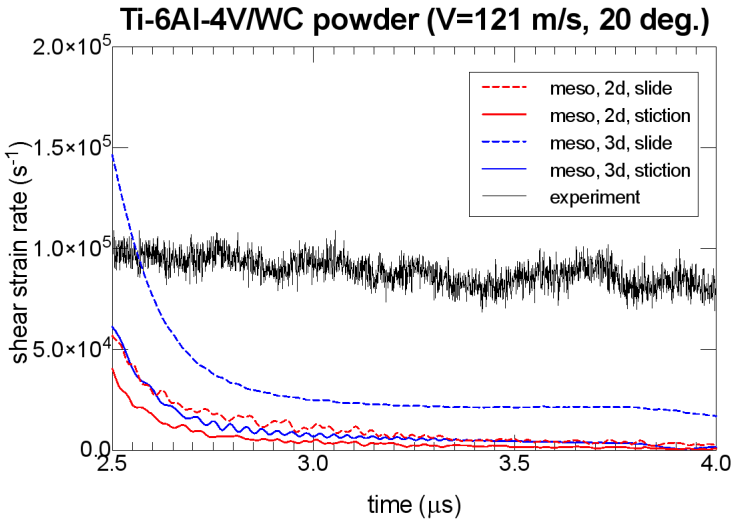

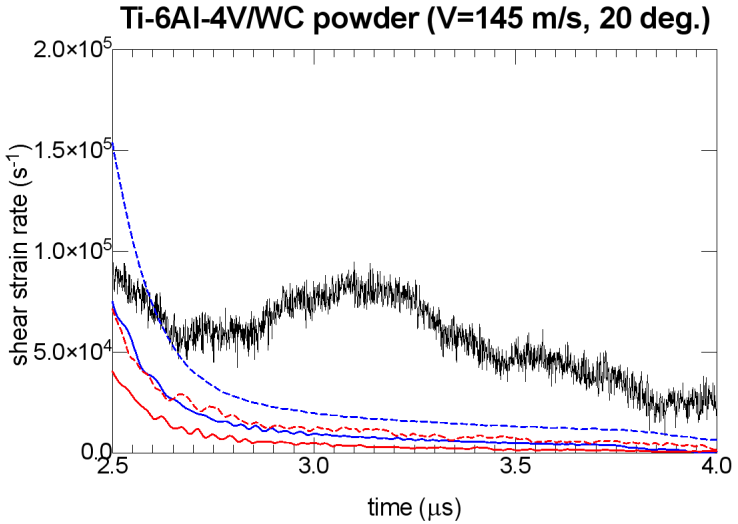

Probing the failure surface of the mesoscale powder model

- Adjust impact velocity and nose angle to generate shear waves of increasing amplitude, while fixing the normal wave amplitude

$$V = \frac{2\sigma_{el}}{\rho_{0,A} C_{L,A}} \left[1 + \left(\frac{C_{L,A}\tau_{el}}{C_{S,A}\sigma_{el}} \right)^2 \right]^{1/2} \quad \text{and} \quad \theta = \tan^{-1}\left(\frac{C_{L,A}\tau_{el}}{C_{S,A}\sigma_{el}} \right)$$

- Stiction simulations (not shown) show increase in transmitted transverse velocity to very high values and unrealistic failure mechanism
- Slide simulations show transmitted transverse velocity is bounded for a given normal stress state
- Both 2D and 3D simulations show increase in transverse velocity bound with increasing normal stress
- Decrease in transverse velocity during flow due to formation of localized shear interfaces in sample

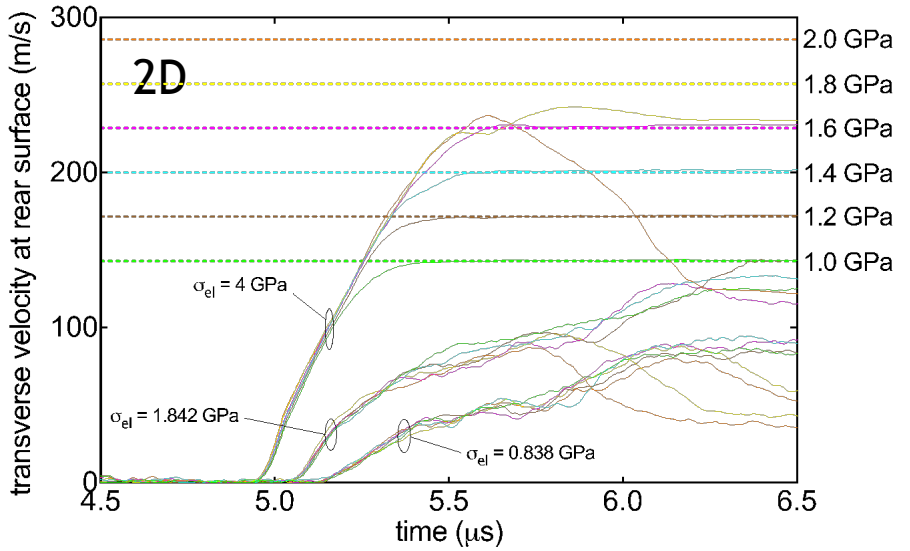

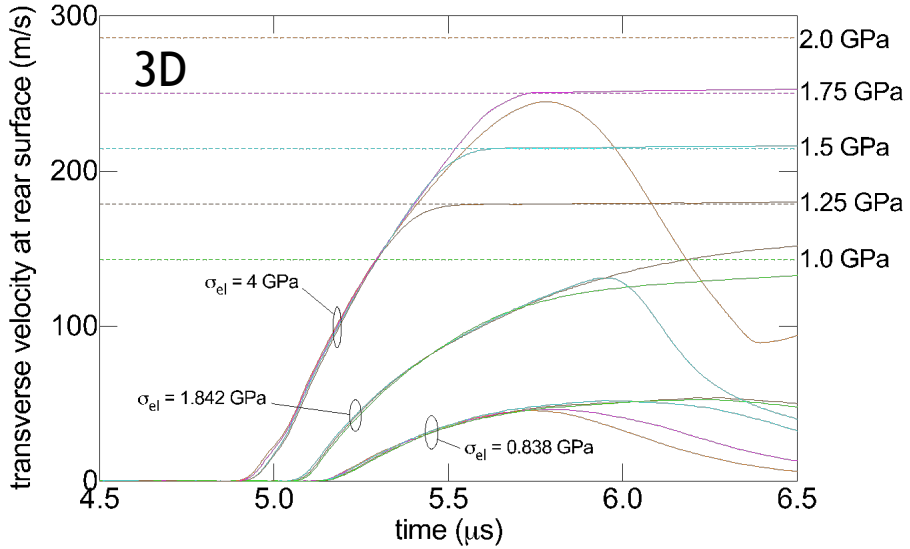

Probing the Shear Failure Surface of the Mesoscale Powder Model

- Adjust V and θ to generate shear waves of increasing amplitude τ_{el}, while keeping normal wave amplitude σ_{el} fixed

$$V = \frac{2\sigma_{el}}{\rho_{0,A} C_{L,A}} \left[1 + \left(\frac{C_{L,A}\tau_{el}}{C_{S,A}\sigma_{el}} \right)^2 \right]^{1/2} \quad \text{and} \quad \theta = \tan^{-1}\left(\frac{C_{L,A}\tau_{el}}{C_{S,A}\sigma_{el}} \right)$$

- Simulations with intergranular sliding show transmitted transverse velocity is bounded, while those with default mixed-cell behavior respond elastically (not shown)
- Transverse velocity increases over time, as grains rearrange, followed in some cases by a drop in velocity indicating the formation of a sliding interface within the sample
- High confinement case, sharp transition from elastic response to formation of sliding interface with increasing τ_{el}
- Very few cells reach fracture criterion, while recovered samples in experiment show evidence of significant grain fracture

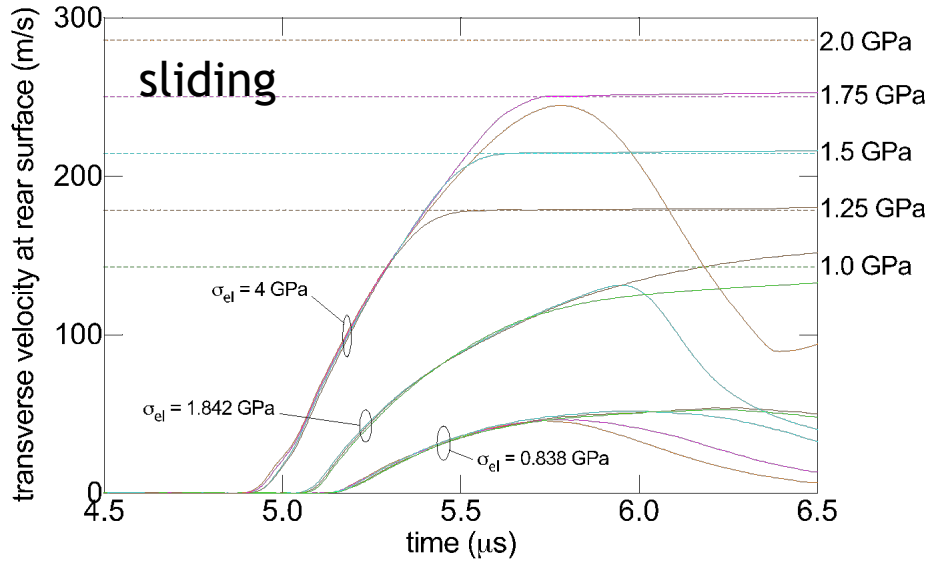

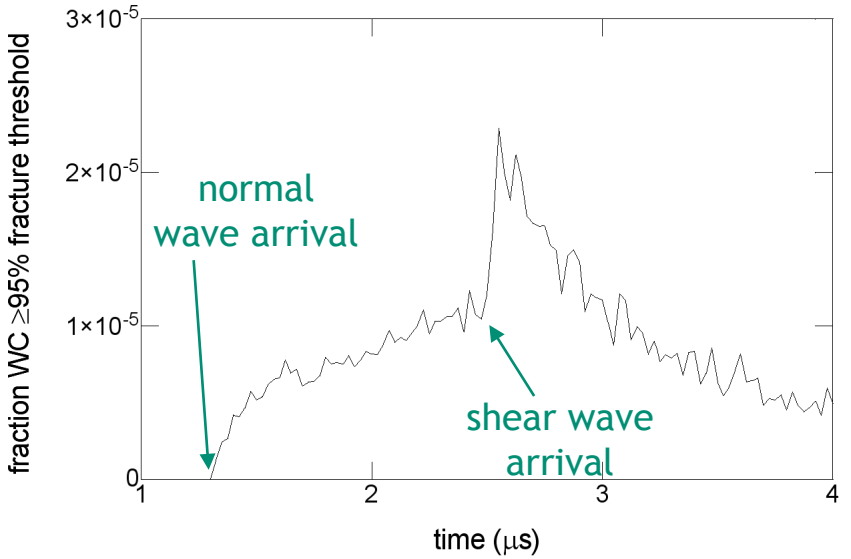

Effect of Intragranular Fracture Strength

- Very few cells reach fracture criterion, while recovered samples in experiment show evidence of significant grain fracture
- Switch to a principal-stress-based fracture criterion and decrease fracture strength from its baseline value of 4 GPa
- Determine upper bounds in normal and transverse velocity histories fixing σ_{el} = 0.838 GPa and varying τ_{el} = 0.25-2 GPa
- Reduction in initial shoulder of normal wave rise with decreasing fracture strength
  - Indicates more compaction during initial rise, which is in better agreement with experiment
  - Snowplow compaction for fracture strength ~0
- Upper bound in transverse velocity decreases with decreasing fracture strength
  - Lower limit for fracture strength 0.25-0.5 GPa
  - Below that the upper bound increases
  - Similar response to high confinement case for fracture strength ~0

normal stress = 0.838 GPa

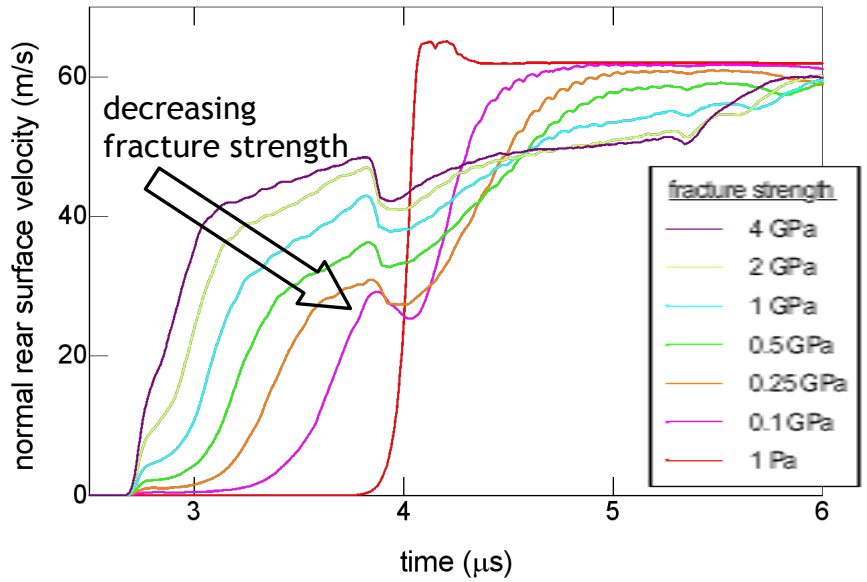

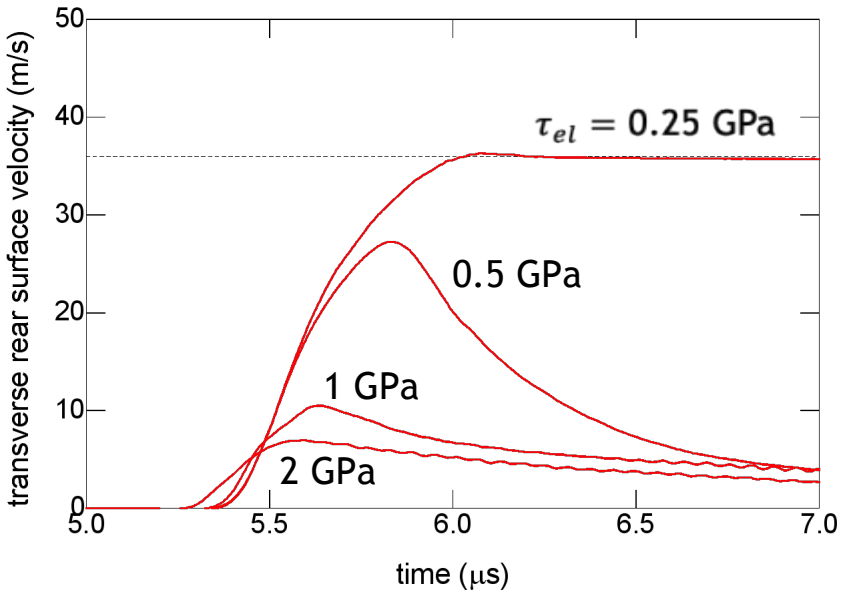

Effect of grain realization (2D)

- Mesoscale powder model for the 2D geometry contains 332 randomly-arranged grains
  - In comparison, the powder model in the 3D geometry contains >7x more (2483) grains
- Ran 2D simulations with different grain realizations
  - Different RNG seeds used to generate the initial grain locations
  - Because some grains are cutoff at the front anvil interface, the actual volume fraction varies from one realization to the next
  - Range of volume fractions is 0.34%
- When the sample is not yielding, there is very little variation in the transverse velocity response among all grain realizations
- However, when the sample is yielding, the variation in transverse velocity becomes quite large after loading by the initial shear wave